GMR
The Original

POLYETHYLENE GLYCOL-BASED ISOLATION AND CHARACTERIZATION OF PLANT-DERIVED EXOSOME-LIKE NANOPARTICLES FROM CARICA PAPAYA L. LEAVES AND THEIR POTENTIAL AS AN ANTICANCER AGENT

Aanya Barman[1]

[1]Oakridge International School, Gachibowli, Hyderabad. Email ID: aanyabarman@gmail.com

ABSTRACT

Plant-derived exosome-like nanoparticles (PDENs) have attracted increasing attention as potential nanocarriers for bioactive compounds because they are biocompatible, have low immunogenicity, and can transport diverse biological cargo. The present study aimed to optimize a polyethylene glycol (PEG)-based isolation method for PDENs from Carica papaya L. leaves and evaluate their in vitro anticancer activity against SCC-131 oral squamous cell carcinoma cells.

Papaya leaf extract was subjected to differential centrifugation followed by PEG-based precipitation using PEG of different molecular weights (3, 6, and 8 kDa) at concentrations of 6%, 8%, and 12% (w/v). The isolated nanoparticles were characterized through protein and lipid quantification, nanoparticle tracking analysis (NTA), and zeta potential measurements. Their cytotoxic activity against SCC-131 cells was evaluated using the MTT assay. Among the tested formulations, 8 kDa PEG at 6% (w/v) was the most favorable isolation condition, with a protein-to-lipid ratio of 2.91. The isolated nanoparticles had a median diameter of 133.4 nm and a mean diameter of 154.0 ± 84.4 nm. The mean zeta potential was −30.73 mV, indicating favorable colloidal stability. MTT assay results showed a progressive reduction in SCC-131 cell viability with increasing PDEN concentration, with a half-maximal inhibitory concentration (IC_{50}) of 34.32 µg/mL. Microscopic observations also revealed cell rounding, loss of adhesion, and increased floating cells, particularly at higher treatment concentrations.

These findings demonstrate the feasibility of PEG-based isolation of C. papaya leaf-derived PDENs and indicate measurable in vitro cytotoxic activity against SCC-131 oral squamous cell carcinoma cells. Further molecular characterization, mechanistic investigations, and in vivo validation are required to establish their therapeutic potential.

KEYWORDS: Carica papaya L.; plant-derived exosome-like nanoparticles (PDENs); polyethylene glycol precipitation; nanoparticle characterization; oral squamous cell carcinoma; SCC-131; MTT cytotoxicity assay; anticancer activity.

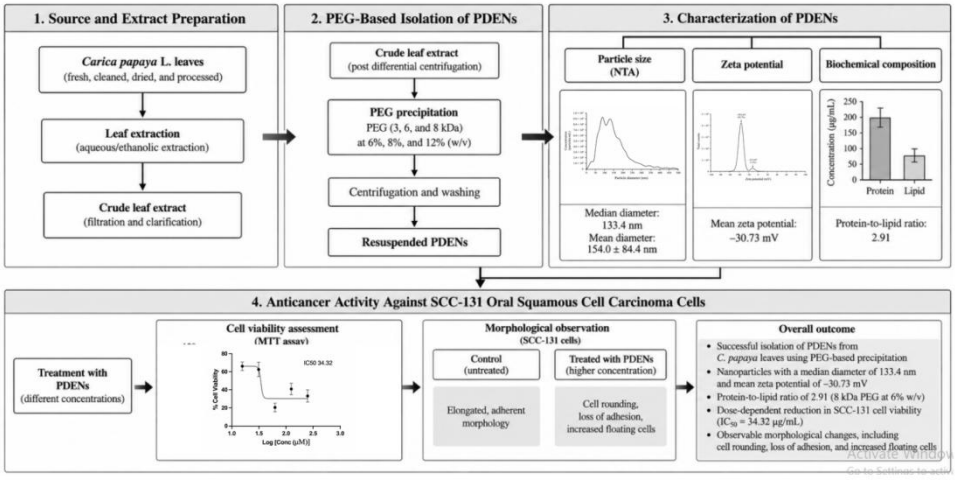


Figure 1: Graphical abstract of the study.

1. INTRODUCTION

Oral squamous cell carcinoma (OSCC) is one of the most prevalent malignancies worldwide, accounting for nearly 90% of the approximately 390,000 new cases of lip and oral cancer reported globally in 2022 (World Health Organization [WHO], 2025). OSCC is a malignant epithelial cancer that originates from the squamous cells lining the oral cavity and primarily affects the tongue, gingiva, buccal mucosa, and floor of the mouth (Eloranta et al., 2024). Persistent exposure to risk factors such as tobacco, alcohol, betel quid chewing, and human papillomavirus infection significantly increases the likelihood of developing OSCC (Tan et al., 2023). Although conventional therapeutic approaches, including surgical resection, radiotherapy, and chemotherapy, as well as targeted therapy and immunotherapy in advanced cases, have improved clinical outcomes, the five-year overall survival rate remains approximately 63%, declining from 83% in early-

stage disease to 38% in advanced-stage disease (Imbesi Bellantoni et al., 2023). These treatments also carry adverse effects, including oral mucositis, nausea, xerostomia, osteoradionecrosis, taste alterations, and immunosuppression (Sankar & Xu, 2023; The Oral Cancer Foundation, 2019). Multidrug resistance further complicates treatment and contributes to therapeutic failure (Ojong et al., 2026). These limitations highlight the need to investigate alternative therapeutic approaches that may selectively target tumor cells while minimizing damage to healthy tissues.

Consequently, natural products have attracted considerable attention in cancer research. An estimated 68% of small-molecule anticancer drugs available between 1940 and 2014 were derived from natural products, highlighting their importance in drug discovery (Ojong et al., 2026). Many plant-derived phytochemicals exhibit cytotoxic activity against malignant cells and may influence tumor-associated biological processes, including cell proliferation, apoptosis, and immune regulation (Ramsridhar et al., 2025). In oral cancer research, plant-derived bioactive compounds have been investigated for their ability to inhibit tumor growth, induce apoptosis, and modulate signaling pathways associated with cancer progression. Compounds such as curcumin, epigallocatechin gallate, and resveratrol have received particular attention for their effects on nuclear factor kappa B (NF-κB) and mitogen-activated protein kinase (MAPK) signaling, which are associated with cancer cell viability, apoptosis, and migration (Kumar & Jha, 2023; Ramsridhar et al., 2025).

Despite their therapeutic potential, bioactive compounds in crude plant extracts may be limited by enzymatic degradation, poor absorption, and low bioavailability. Consequently, only a proportion of these compounds may reach the target tissue at concentrations sufficient to produce the desired biological effect. Plant-derived exosome-like nanoparticles (PDENs) have emerged as a potential approach to addressing these limitations (Calzoni et al., 2024). PDENs are lipid bilayer-enclosed nanovesicles, typically ranging from 50 to 500 nm in diameter, that are naturally released by plant cells (Rider et al., 2016; Calzoni et al., 2024). They are structurally analogous to mammalian exosomes and can carry diverse biological cargo, including proteins, lipids, vitamins, metabolites, and microRNAs (Liu et al., 2025; Iriawati et al., 2024). Encapsulating these constituents within a lipid bilayer may protect them from degradation and improve delivery to recipient cells. Compared with certain synthetic nanocarriers and animal-derived extracellular vesicles, PDENs may also offer advantages in biocompatibility, low immunogenicity, biological versatility, and scalable production from plant sources (Alzahrani et al., 2023; Ramsridhar et al., 2025).

Anticancer activity has been reported for PDENs isolated from several dietary plant sources. Grape-derived nanoparticles have shown concentration-dependent inhibition of the triple-negative breast cancer cell line MDA-MB-231, reducing cell viability to about 70% of the control at the highest tested particle concentration (Shkryl et al., 2024). Similarly, ginger exosome-like nanoparticles have been reported to induce concentration-dependent cytotoxicity in MDA-MB-231 cells, alongside apoptosis-associated changes, cell-cycle arrest, and reduced cell migration and colony formation (Anusha et al., 2023). Extracellular vesicles derived from bitter melon have also shown activity against OSCC cell lines, including inducing S-phase cell-cycle arrest and apoptosis (Yang et al., 2021). These findings support further investigation of plant-derived nanovesicles as potential platforms for anticancer applications.

Carica papaya L. is a medicinal plant widely used in traditional medicine, particularly in tropical and subtropical regions such as India. Although papaya is recognized for its proteolytic enzymes, including papain, it also contains flavonoids, phenolic compounds, alkaloids, and other bioactive constituents associated with antimicrobial, antioxidant, and anti-inflammatory properties (Hariono et al., 2021; Iriawati et al., 2024; Sharma et al., 2022). Preparations derived from papaya leaves and fruits have shown antiproliferative and apoptosis-inducing effects in various cancer models, including breast and ovarian cancer (Nisa et al., 2016; Priyadurairaj et al., 2020; Rebeea et al., 2025). These effects have been associated with the modulation of genes and signaling pathways involved in tumor progression, including Bcl-2, Bcl-xL, CDK4, Cyclin D1, PI3K/Akt, and Wnt/β-catenin (Patel et al., 2024; Singh et al., 2020; Lee et al., 2021; Ajax et al., 2025). Because PDENs may retain biomolecules from their parent plant tissues, nanoparticles isolated from papaya leaves could transport bioactive phytochemicals. Although researchers have isolated and characterized papaya-derived PDENs for their potential anti-inflammatory applications, the anticancer activity of leaf-derived PDENs against oral squamous cell carcinoma remains insufficiently investigated, providing a rationale for the present study.

The isolation method also influences PDENs' biological properties, affecting nanoparticle yield, purity, and structural integrity (Ojong et al., 2026). Several techniques have been employed for extracellular vesicle isolation, including ultracentrifugation, size-exclusion chromatography, ultrafiltration, immunoprecipitation, microfluidics, and polymer-based precipitation (Farhang Aliakbari et al., 2024). Ultracentrifugation separates particles by size and density using high centrifugal forces (Li et al., 2017). Although widely used, this method may require specialized, expensive equipment, considerable processing time, and conditions such as use of high force, that can compromise vesicle stability. Polyethylene glycol (PEG)-based precipitation offers an alternative approach in which PEG interacts with water molecules, promoting nanoparticle aggregation and precipitation that can then be recovered by centrifugation (Rider et al., 2016). However, PEG molecular weight and concentration can influence particle recovery, purity, and the co-precipitation of soluble proteins. Therefore, isolation conditions must be optimized based on the biological source and intended downstream application (Marzouk et al., 2025).

Given the reported anticancer properties of plant-derived nanovesicles and the bioactive phytochemical composition of C. papaya, this study aimed to optimize a PEG-based isolation protocol for PDENs from C. papaya L. leaves and evaluate their in vitro anticancer activity against SCC-131 oral squamous cell carcinoma cells. The study compared PEG molecular weights and concentrations, characterized the isolated nanoparticles using biochemical and physicochemical analyses, and evaluated their effects on cancer cell viability with the MTT assay.

2. MATERIALS AND METHODS

2.1. Study Design and Isolation Approach

Plant-derived exosome-like nanoparticles (PDENs) were isolated from Carica papaya L. leaves using polyethylene glycol (PEG)-based precipitation, with modifications to the PEG molecular weights and concentrations. The isolation procedure

was based on the PEG-mediated method described by Kalarikkal et al. (2020), while the differential centrifugation steps used to remove cellular debris were adapted from Théry et al. (2006).
The experimental workflow included papaya leaf collection and processing, differential centrifugation, PEG-mediated nanoparticle precipitation, biochemical and physicochemical characterization, and in vitro evaluation of the cytotoxic effects of the isolated PDENs against SCC-131 oral squamous cell carcinoma cells.

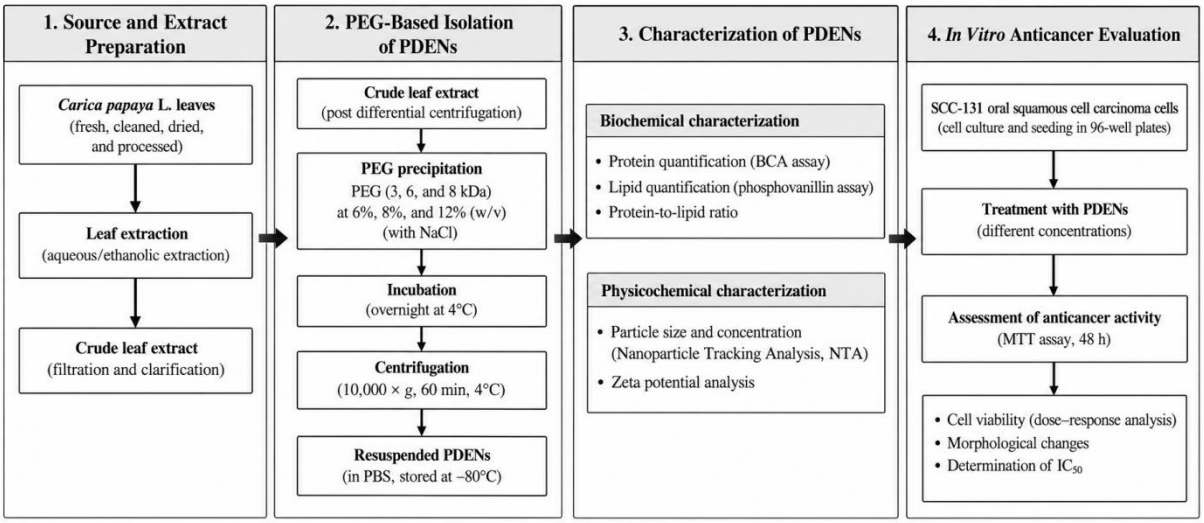


Figure 2. Experimental workflow for the isolation, characterization, and in vitro evaluation of plant-derived exosome-like nanoparticles from Carica papaya L. leaves.

2.2. Collection and Processing of Papaya Leaves

Fresh Carica papaya L. leaves were obtained from a local farm and washed thoroughly with 70% ethanol to minimize surface contaminants. The leaves were deveined and ground using a juicer to obtain the leaf extract. The resulting extract was filtered through muslin cloth repeatedly to remove fibrous material and coarse particulates before further processing. Approximately 100 mL of the filtered extract was used for subsequent isolation.

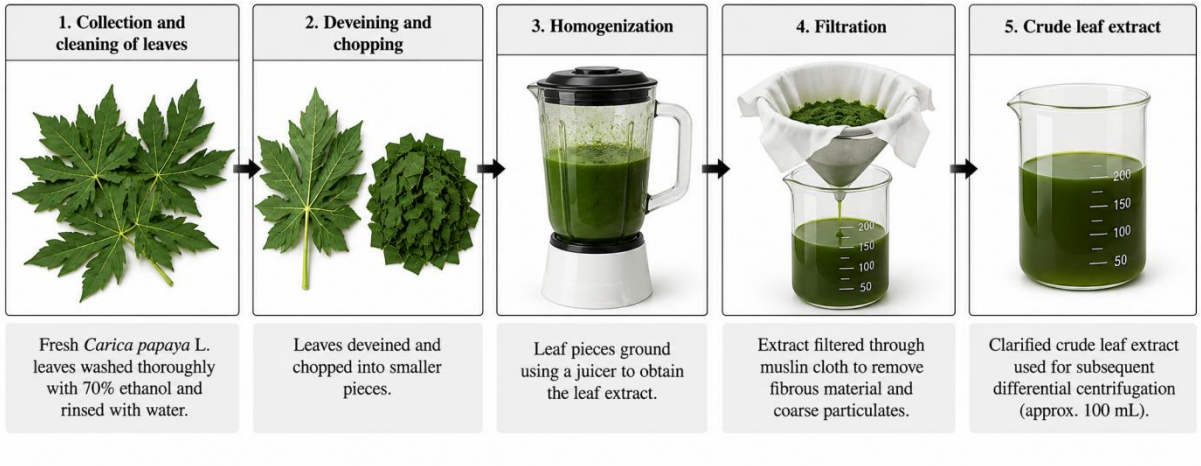


Figure 3. Preparation of Carica papaya L. leaf extract prior to differential centrifugation.

2.3. Isolation of Papaya Leaf-Derived PDENs

2.3.1. Differential Centrifugation

The filtered papaya leaf extract underwent sequential differential centrifugation to remove cells, large debris, and organelle fragments before PEG precipitation. We centrifuged 100 mL of extract sequentially at 3,000 × g for 10 min, 2,000 × g for 10 min, and 10,000 × g for 30 min. All centrifugation steps were performed at 4°C.
Following each centrifugation step, the supernatant was carefully transferred into fresh centrifuge tubes without disturbing the pellet. The resulting clarified supernatant was used for PEG-based precipitation. This preliminary clarification procedure followed the approach adapted from Théry et al. (2006).

2.3.2. Preparation of PEG Precipitation Solutions

PEG solutions of three molecular weights, 3, 6, and 8 kDa, were evaluated at concentrations of 6%, 8%, and 12% (w/v). The preparation included 0.58 g of sodium chloride per 50 mL of solution. We assessed PEG-based precipitation conditions according to the isolation approach described by Kalarikkal et al. (2020), varying PEG molecular weight and concentration to compare the resulting preparations. PEG precipitation was also considered in the context of the concentration-dependent recovery and co-precipitation concerns discussed by Marzouk et al. (2025).

2.3.3. PEG-Mediated Precipitation and Recovery

The clarified papaya leaf supernatant was divided equally between two 50-mL Falcon centrifuge tubes. Each portion was mixed with an equal volume of the corresponding PEG solution (1:1). The mixtures were incubated overnight at 4°C to promote PDEN precipitation.

Following incubation, the samples were centrifuged at 10,000 × g for 60 min at 4°C. The resulting pellets were resuspended in 5 mL of phosphate-buffered saline (PBS) and stored at −80°C until further characterization and biological analysis. Centrifugation was performed using an Eppendorf 5810R refrigerated centrifuge fitted with an F-34-6-38 rotor (Eppendorf, Hamburg, Germany).

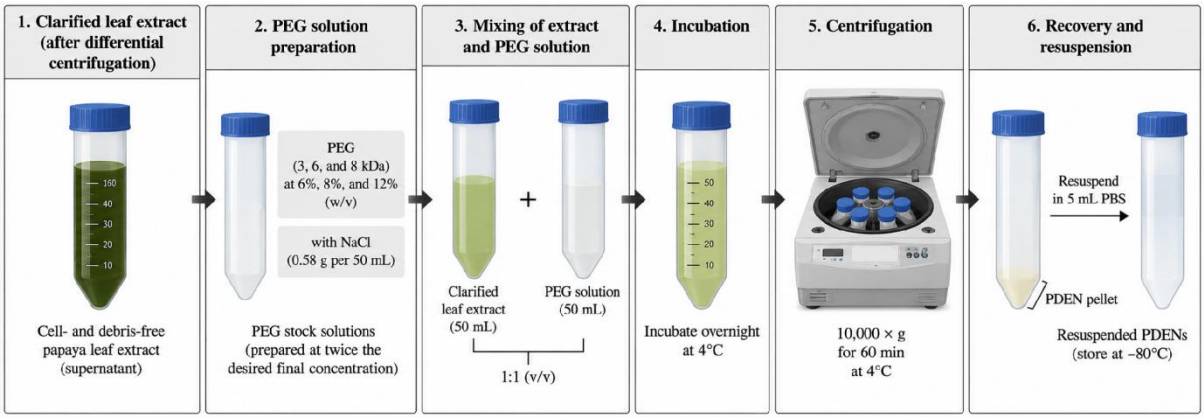


Figure 4: PEG-mediated precipitation and recovery of papaya leaf-derived PDEN preparations.

Table 1. PEG-Based Isolation Conditions Evaluated for Papaya Leaf PDENs.

PEG molecular weight	PEG concentration (w/v)	Sample designation
3 kDa	6%	3K PEG 6%
3 kDa	8%	3K PEG 8%
3 kDa	12%	3K PEG 12%
6 kDa	6%	6K PEG 6%
6 kDa	8%	6K PEG 8%
6 kDa	12%	6K PEG 12%
8 kDa	6%	8K PEG 6%
8 kDa	8%	8K PEG 8%
8 kDa	12%	8K PEG 12%

2.4. Biochemical Characterization of PDEN Preparations

2.4.1. Protein Quantification

The protein concentration of the isolated papaya leaf PDENs was measured using the bicinchoninic acid (BCA) protein assay according to the manufacturer's protocol (Thermo Fisher Scientific, n.d.).

We prepared a bovine serum albumin (BSA) standard curve by serially diluting 80 µL of BSA stock into six clean vials, using PBS as the control. The BCA working reagent was prepared by mixing Reagent A and Reagent B at a 50:1 ratio. Aliquots of 5 µL of each standard and sample were transferred to a 96-well plate, and the plate was incubated at 37°C for 30 min.

Protein concentrations were assessed for all nine PEG formulations: 3K PEG at 6%, 8%, and 12%; 6K PEG at 6%, 8%, and 12%; and 8K PEG at 6%, 8%, and 12%. We measured samples in duplicate using a microplate reader at 560 nm. The BSA standard curve was used to calculate protein concentrations.

After the initial characterization indicated that the 8K PEG 6% (w/v) condition was suitable for subsequent work, a new batch was prepared in a larger quantity. Protein quantification of this preparation was repeated using the BCA assay.

2.4.2. Lipid Quantification

We determined the total lipid content of the PDEN preparations using the phosphovanillin assay. The lipid standard was 1,2-dioleoyl-sn-glycero-3-phosphocholine (DOPC; Avanti Polar Lipids Inc., Alabama, USA).

For each standard or PDEN sample, 40 µL was combined with 200 µL of 96% sulfuric acid (H_2SO_4). The mixtures were heated at 90°C in a dry bath for 20 min, then cooled to room temperature. A volume of 120 µL of phosphovanillin reagent, prepared by dissolving 50 mg of vanillin in 50 mL of 17% phosphoric acid (H_3PO_4; Sigma, Missouri, USA), was then added.

We transferred 180 µL of the resultant reaction mixture to the corresponding wells of a 96-well plate and incubated it at 37°C for 1 h. We measured absorbance at 540 nm using a microplate reader. Total lipid concentrations were calculated from the lipid-standard curve.

2.4.3. Protein-to-Lipid Ratio

The protein-to-lipid ratio was used to compare the biochemical composition of the preparations recovered under different PEG conditions. This parameter was calculated from the measured protein and lipid concentrations for each preparation:
[{Protein-to-lipid ratio} ={Protein concentration}\{Lipid concentration}]
The ratio was interpreted as a comparative compositional parameter rather than a definitive measure of vesicle purity, consistent with the use of protein-to-lipid measurements in extracellular-vesicle characterization (Osteikoetxea et al., 2015).

2.5. Physicochemical Characterization of PDENs

2.5.1. Nanoparticle Tracking Analysis

The particle-size distribution and particle concentration of the isolated papaya leaf nanoparticles were assessed using a NanoSight instrument (Malvern Ltd., Malvern, UK). The sample was diluted with HPLC-grade water in two sequential dilution steps. First, 10 µL of the PDEN sample was diluted to 1 mL. Subsequently, 10 µL of this dilution was added to 990 µL of HPLC-grade water. Finally, a third dilution was performed by adding 100 µL of the previous solution to 900 µL of HPLC- grade water, yielding a total dilution factor of 1:100,000.
The final diluted sample was loaded into the instrument, and the manufacturer's recommended acquisition settings were used to record the Brownian motion of individual particles for 30 s. The recordings were analyzed using NTA software, version 2.3 Build 0025, to determine particle-size distribution and particle concentration.

2.5.2. Zeta Potential Analysis

The zeta potential of the isolated papaya leaf-derived plant-derived exosome-like nanoparticles (PDENs) was evaluated to assess their surface charge characteristics. The electrophoretic mobility and zeta potential distributions of the optimized preparation obtained using 8 kDa PEG at 6% (w/v) were analyzed, and the mean zeta potential and particle concentration were recorded. Measurements were reported at 25°C, and the zeta potential distribution was used to characterize the surface-charge properties of the isolated nanoparticle population.

2.6. Preparation and Culture of the SCC-131 Cell Line

SCC-131 oral squamous cell carcinoma cells were cultured according to the procedure attributed to Vikas and Anil (2020). The complete culture medium consisted of Dulbecco's Modified Eagle Medium (DMEM) supplemented with 10% fetal bovine serum (FBS) and 1% penicillin–streptomycin (PS). The medium was pre-warmed to 37°C before use, and cell-culture procedures were conducted under sterile conditions in a Class II biological safety cabinet.
Cryopreserved SCC-131 cells, stored at −80°C, were rapidly thawed in a 37°C water bath for approximately 1–2 min. The thawed cell suspension was transferred to a sterile 15-mL centrifuge tube and centrifuged at 1,000 rpm for 5 min to remove the dimethyl sulfoxide (DMSO) cryoprotectant. After removal of the supernatant, the cell pellet was resuspended in 5 mL of fresh complete culture medium and transferred to a T25 tissue-culture flask.
The cells were maintained at 37°C in a humidified atmosphere containing 5% CO_2. After 24 h, cell attachment and morphology were examined using an inverted microscope. Cultures were then maintained for three days, with daily microscopic observation, until appropriate cell growth was achieved.

2.7. Seeding of SCC-131 Cells

After establishment of the culture, the spent medium was removed, and the cell monolayer was gently washed with PBS. The cells were detached by adding 1 mL of trypsin and incubating for 3–4 min at 37°C. The trypsin reaction was stopped by adding 4 mL of complete culture medium, and the suspension was gently pipetted to produce a uniform cell suspension. The suspension was transferred to a sterile centrifuge tube and centrifuged at 1,000 rpm for 5 min. The supernatant was removed, and the cell pellet was resuspended in 1 mL of complete culture medium.
Cell concentration was determined using a Neubauer hemocytometer. A seeding density of 8,000 cells per well was used. Based on the reported cell concentration of 1,003,000 cells, we combined 559 µL of cell suspension with 6,641 µL of complete culture medium to prepare the required suspension. We dispensed the suspension into three 96-well plates in triplicate using a multichannel pipette.
To reduce evaporation-related edge effects, 100 µL of sterile PBS was added to the edge wells, following the approach described by Mansoury et al. (2021). The plates were incubated for 48 h at 37°C in a humidified atmosphere containing 5% CO_2 to permit cell attachment and recovery before PDEN treatment.

2.8. MTT Cytotoxicity Assay

The cytotoxic activity of papaya leaf PDENs against SCC-131 cells was evaluated using the MTT assay. The PDEN stock was diluted in complete culture medium to obtain treatment concentrations of 250, 125, 62.5, 31.25, and 15.625 µg/mL, based on protein concentration. A medium-only control and a PBS control were included to distinguish treatment effects from potential vehicle-related effects.
The culture plates were examined using an inverted microscope after 18–24 h to assess cell attachment and general cell condition. We then carefully withdrew the culture medium from each well under sterile conditions, avoiding disturbance of the cell layer. A 10-µL aliquot of the respective PDEN dilution was added to each treatment well in triplicate. Control wells received 10 µL of complete culture medium or PBS, as applicable. We incubated the cells for an additional 48 h at 37°C in a humidified atmosphere containing 5% CO_2. This 48-h exposure period matches the treatment period cited in the source manuscript (Dziedzic et al., 2016).
After treatment, we added 20 µL of MTT solution (5 mg/mL) to each well. We incubated the plates in the dark for 4 h to allow insoluble formazan crystals to form. The supernatant was carefully removed without disturbing the crystals, which were dissolved in 200 µL of DMSO. We measured absorbance at 540 nm using a microplate reader.
Cell viability was determined by comparing the absorbance of treated samples with that of the untreated control. A dose–response curve was generated to estimate the half-maximal inhibitory concentration (IC_{50}).

Table 2. Summary of Principal Experimental and Analytical Conditions.

Experimental procedure	Working Conditions
Leaf-extract processing	Fresh leaves washed with 70% ethanol, deveined, ground using a juicer, and filtered through muslin cloth.
Differential centrifugation	3,000 × g for 10 min; 2,000 × g for 10 min; 10,000 × g for 30 min; 4°C
PEG precipitation	PEG of 3, 6, and 8 kDa; concentrations of 6%, 8%, and 12% (w/v)
PDEN precipitation	Overnight incubation at 4°C, followed by centrifugation at 10,000 × g for 60 min at 4°C
Final PDEN suspension	Resuspended in 5 mL PBS and stored at −80°C
Protein assay	BCA assay; 5 µL of standards/samples; reagent A at 50:1; 30 min at 37°C; absorbance at 560 nm; duplicate measurements
Lipid assay	Phosphovanillin assay using DOPC standard; 200 µL of 96% H_2SO_4 and 40 µL of sample/standard; 90°C for 20 min; 120 µL of reagent; 1 h at 37°C; absorbance at 540 nm
Nanoparticle tracking analysis	NanoSight instrument; 30-s recording; NTA software version 2.3 Build 0025
Cell-culture medium	DMEM supplemented with 10% FBS and 1% penicillin–streptomycin
Cell-seeding density	8,000 cells per well in 96-well plates; triplicate wells; sterile PBS added to edge wells
PDEN treatment concentrations	250, 125, 62.5, 31.25, and 15.625 µg/mL, plus medium-only and PBS controls
Treatment duration	48 h at 37°C and 5% CO_2
MTT assay	20 µL MTT solution at 5 mg/mL; 4 h in the dark; 200 µL DMSO to dissolve formazan; absorbance at 540 nm
Statistical/data analysis	GraphPad Prism version 11; dose–response curve, IC_{50} estimation, and presentation as mean ± SEM

2.9. Statistical and Data Analysis

Cell-viability measurements from the MTT assay were tabulated to assess the effects of Carica papaya L. leaf PDENs on SCC-131 cells. GraphPad Prism version 11 was used to generate the dose–response curve, calculate the IC_{50} value, and present the results as mean ± standard error of the mean (SEM).

3. RESULTS

3.1. Comparative Evaluation of PEG-Based PDEN Isolation Conditions

Protein and lipid quantification was used to compare the nine PEG-based precipitation conditions evaluated for the isolation of Carica papaya L. leaf-derived plant-derived exosome-like nanoparticles (PDENs). Protein concentrations ranged from 2,074.5 to 9,689.5 µg/mL, while lipid concentrations ranged from 660.3 to 2,167.0 µg/mL. The calculated protein-to-lipid (P/L) ratios ranged from 2.76 to 4.47 (Table 3).

The 3 kDa PEG preparation at 6% (w/v) yielded the lowest measured protein concentration (2,074.5 µg/mL), whereas the 8 kDa PEG preparation at 12% (w/v) yielded the highest (9,689.5 µg/mL). The 12% formulations also showed relatively high P/L ratios, ranging from 4.36 to 4.47. The 8 kDa PEG formulation at 6% (w/v) produced a protein concentration of 4,004.5 µg/mL, a lipid concentration of 1,376.4 µg/mL, and a P/L ratio of 2.91.

The lowest P/L ratio was 2.76 for 6 kDa PEG at 6% (w/v), followed by 2.91 for 8 kDa PEG at 6% (w/v). Although the 8 kDa PEG 6% formulation was subsequently selected for further characterization, the P/L ratio alone does not establish it as the formulation with the lowest ratio. The selection should therefore be interpreted in the context of the combined characterization results and the intended subsequent experiments.

Table 3. Protein and Lipid Concentrations and Protein-to-Lipid Ratios of PDEN Preparations Obtained Using Different PEG Formulations.

PEG formulation	Protein concentration (µg/mL)	Lipid concentration (µg/mL)	P/L ratio
3 kDa PEG, 6%	2,074.5	660.3	3.14
3 kDa PEG, 8%	4,029.5	1,200.9	3.36
3 kDa PEG, 12%	7,079.0	1,770.3	4.47
6 kDa PEG, 6%	2,877.0	1,041.4	2.76
6 kDa PEG, 8%	3,417.0	1,152.6	2.96
6 kDa PEG, 12%	8,307.0	1,906.4	4.36
8 kDa PEG, 6%	4,004.5	1,376.4	2.91
8 kDa PEG, 8%	4,469.5	1,381.4	3.24
8 kDa PEG, 12%	9,689.5	2,167.0	4.47

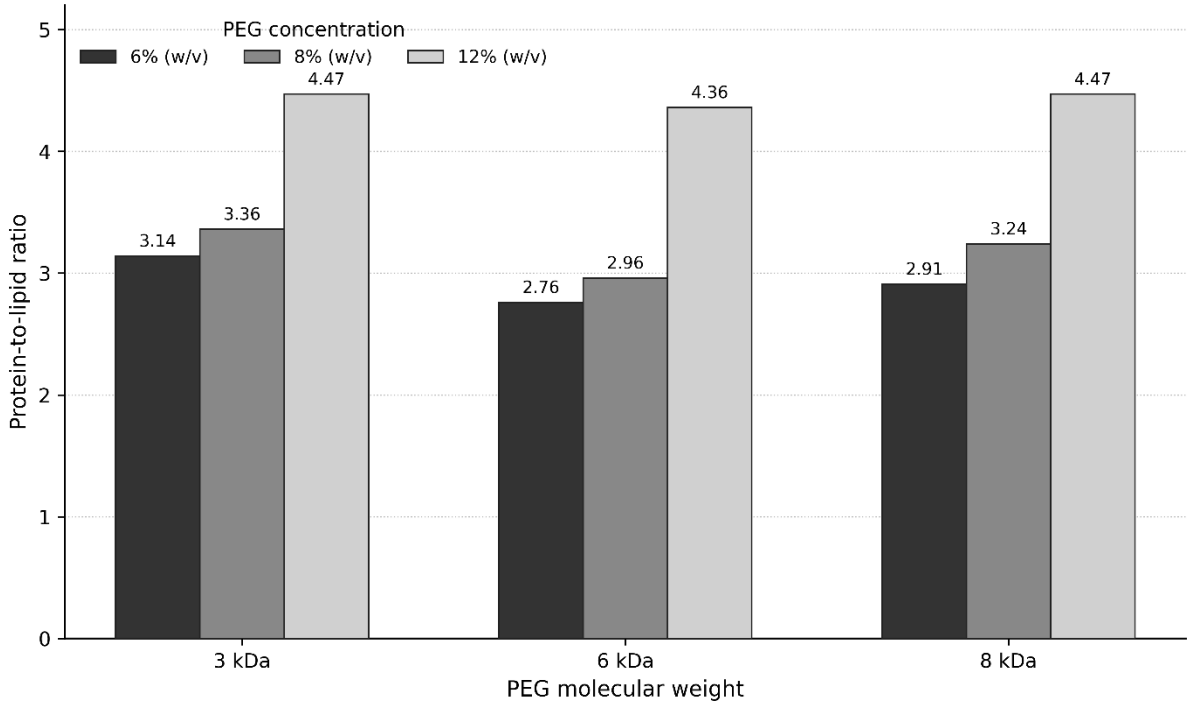


Figure 5. Protein-to-lipid ratios of papaya leaf-derived PDEN preparations obtained using different PEG molecular weights and concentrations.

3.2. Nanoparticle Tracking Analysis of the Selected PDEN Preparation

Nanoparticle tracking analysis (NTA) was used to characterize the size distribution and particle concentration of the preparation selected for further evaluation. The reported median particle diameter (D50/X50) was 133.4 nm, while the mean particle diameter was 154.0 ± 84.4 nm. The D10 and D90 values were 69.9 and 254.8 nm, respectively, yielding a reported span value of 1.4 (Table 4).

Peak analysis identified two predominant particle-size populations, centered at 127.6 nm and 97.8 nm. These were reported to represent 67.0% and 33.0% of the particle population, respectively. Their respective full widths at half maximum (FWHM) were 82.6 nm and 42.3 nm.

The measured particle concentration was reported as (2.6 \times 10^8) particles/mL, corresponding to a dilution-corrected concentration of (2.6 \times 10^{13}) particles/mL in the original preparation. These measurements describe a nanoscale particle population with a distribution of particle sizes rather than a single uniform diameter.

Table 4. Nanoparticle Tracking Analysis of Carica papaya L. Leaf-Derived PDENs.

Parameter	Reported value
Mean particle diameter	154.0 nm
Standard deviation of diameter	84.4 nm
Median diameter (D50/X50)	133.4 nm
D10	69.9 nm
D90	254.8 nm
Span	1.4
Measured particle concentration	(2.6 \times 10^8) particles/mL
Dilution-corrected particle concentration	(2.6 \times 10^{13}) particles/mL
Major peak diameter	127.6 nm
Major peak concentration	(8.9 \times 10^6) particles/mL
Major peak FWHM	82.6 nm
Major peak population	67.0%
Minor peak diameter	97.8 nm
Minor peak concentration	(9.0 \times 10^6) particles/mL
Minor peak FWHM	42.3 nm
Minor peak population	33.0%

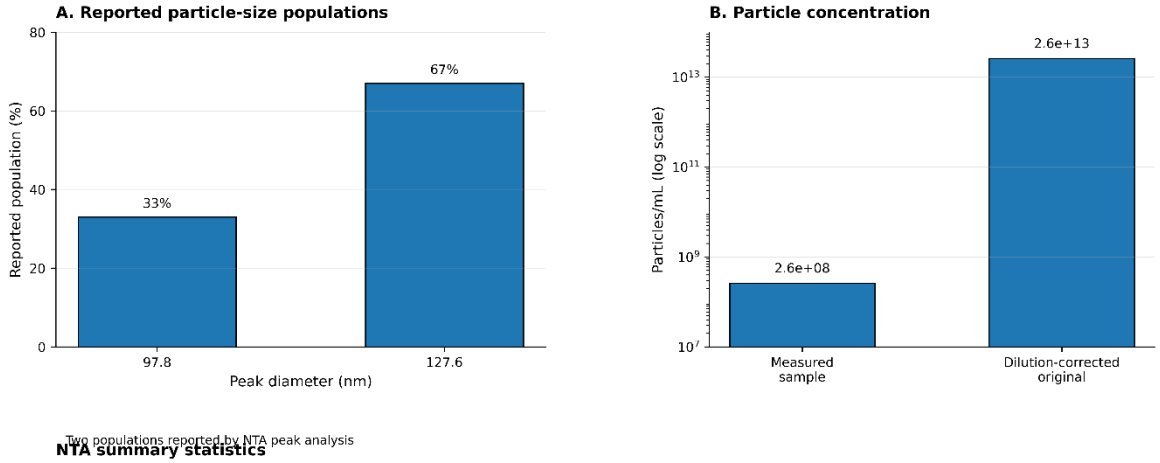


Figure 6. Particle-size distribution and concentration of papaya leaf-derived PDENs determined by nanoparticle tracking analysis.

3.3. Zeta Potential Analysis

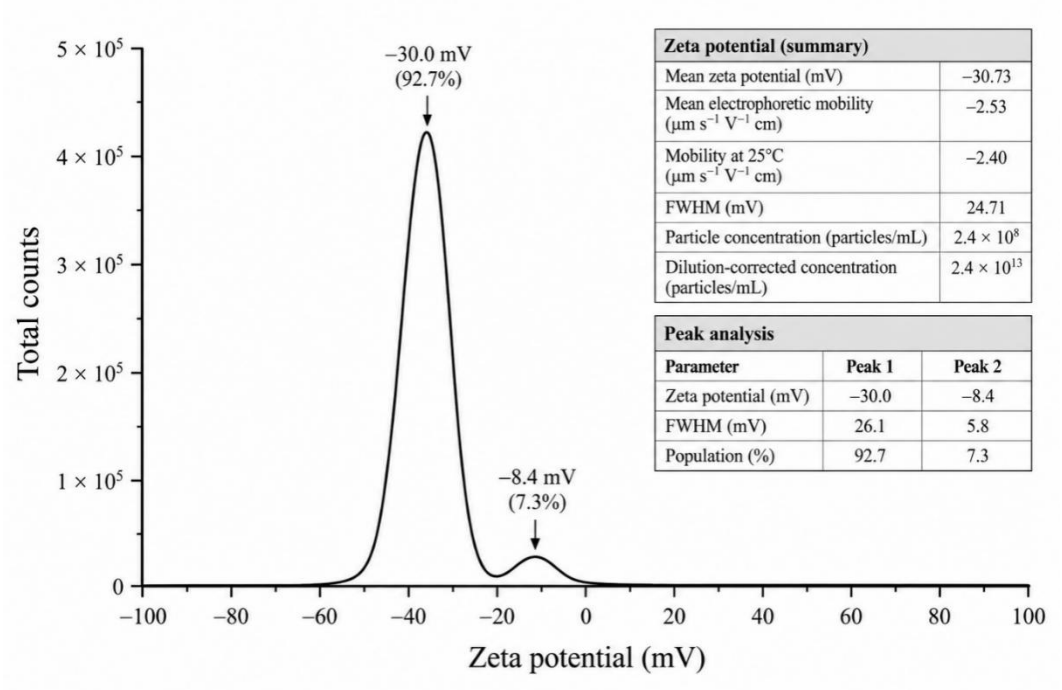
Zeta potential analysis of the selected preparation showed a mean zeta potential of −30.73 mV, corresponding to a reported mean electrophoretic mobility of −2.53 µm s^{-1} V^{-1} cm. The zeta potential distribution had a reported FWHM of 24.71 mV.

Peak analysis identified a predominant population centered at −30.0 mV, accounting for 92.7% of the reported particle population, and a secondary population centered at −8.4 mV, accounting for 7.3% (Table 5). The measured particle concentration was (2.4 \times 10^8) particles/mL, with a reported dilution-corrected concentration of (2.4 \times 10^{13}) particles/mL.

The predominance of the negative-potential population indicates that most of the measured particles exhibited a similar surface-charge profile under the reported measurement conditions. The mean zeta potential is also consistent with the interpretation that electrostatic repulsion may contribute to dispersion stability. However, zeta potential alone does not establish nanoparticle identity, purity, or long-term stability.

Table 5. Zeta Potential Characteristics of Carica papaya L. Leaf-Derived PDENs.

Parameter	Reported value
Mean zeta potential	−30.73 mV
Mean electrophoretic mobility	−2.53 µm s^{-1} V^{-1} cm
Mobility reported at 25°C	−2.40 µm s^{-1} V^{-1} cm
Zeta potential FWHM	24.71 mV
Measured particle concentration	(2.4 \times 10^8) particles/mL
Dilution-corrected particle concentration	(2.4 \times 10^{13}) particles/mL
Major peak zeta potential	−30.0 mV
Major peak FWHM	26.1 mV
Major peak population	92.7%
Minor peak zeta potential	−8.4 mV
Minor peak FWHM	5.8 mV
Minor peak population	7.3%



Zeta potential (summary)	
Mean zeta potential (mV)	−30.73
Mean electrophoretic mobility (μm s^{-1} V^{-1} cm)	−2.53
Mobility at 25°C (μm s^{-1} V^{-1} cm)	−2.40
FWHM (mV)	24.71
Particle concentration (particles/mL)	2.4×10^8
Dilution-corrected concentration (particles/mL)	2.4×10^{13}

Peak analysis		
Parameter	**Peak 1**	**Peak 2**
Zeta potential (mV)	−30.0	−8.4
FWHM (mV)	26.1	5.8
Population (%)	92.7	7.3

Figure 7. Zeta potential distribution of papaya leaf-derived PDENs obtained using the selected 8 kDa PEG, 6% (w/v) precipitation condition.

3.4. Protein Quantification of the Freshly Prepared 8 kDa PEG 6% Formulation

Following the initial biochemical and physicochemical characterization, a new batch was prepared using the selected 8 kDa PEG 6% (w/v) condition to provide material for subsequent biological experiments.

Table 6. Reported Protein Quantification for the Fresh 8 kDa PEG 6% (w/v) PDEN Preparation.

Measurement	Reported value
Protein concentration	13,314.5 μg/mL
Optical density, minus blank	2.67

3.5. Effects of Papaya Leaf-Derived PDENs on SCC-131 Cell Viability

The in vitro cytotoxic activity of the selected papaya leaf-derived PDEN preparation was evaluated against SCC-131 oral squamous cell carcinoma cells using the MTT assay. The investigation reports treatment concentrations of 15.625, 31.25, 62.5, 125, and 250 μg/mL, along with medium-only and PBS controls.

The reported cell viability values were 66.11% at 15.625 μg/mL, 62.50% at 31.25 μg/mL, 20.59% at 62.5 μg/mL, 40.85% at 125 μg/mL, and 33.11% at 250 μg/mL. Viability was reported as 100.00% for the medium control and 114.03% for the PBS control (Table 7).

The reported measurements show that several PDEN-treated groups had lower viability than the medium control. However, the values do not form a strictly concentration-dependent decline: viability at 62.5 μg/mL is lower than that at both 125 and 250 μg/mL. The results therefore indicate reduced viability in treated cells, but the non-monotonic pattern should be considered when interpreting the dose–response relationship.

The source manuscript reports an IC_{50} of 34.32 μg/mL, derived from the dose–response analysis. This estimate should be verified against the underlying replicate-level viability measurements and the fitted regression model, particularly because the recorded value at 62.5 μg/mL departs from a monotonic response.

Table 7. Reported MTT Absorbance and Cell Viability of SCC-131 Cells Following Treatment with Papaya Leaf-Derived PDENs.

Treatment concentration	Absorbance at 540 nm	Reported cell viability (%)
250 μg/mL	0.672	33.11
125 μg/mL	0.830	40.85
62.5 μg/mL	0.418	20.59
31.25 μg/mL	1.270	62.50
15.625 μg/mL	1.342	66.11
Medium-only control (0 μg/mL)	2.031	100.00
PBS control	2.316	114.03

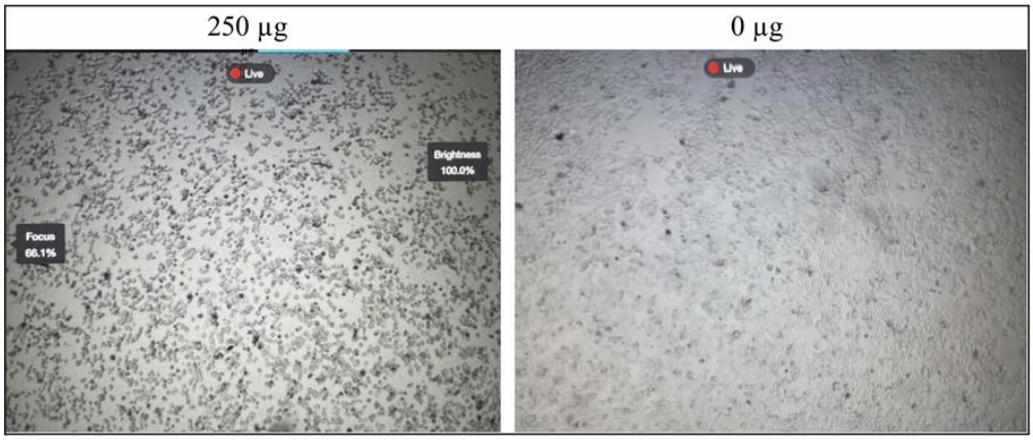


Figure 8. Morphological changes in SCC-131 oral squamous cell carcinoma cells following treatment with papaya leaf-derived PDENs at different concentrations, compared with the untreated control.

3.6. Relationship Between PDEN Concentration and Cell Viability

Pearson's correlation analysis yielded a reported coefficient of −0.630 for the relationship between PDEN concentration and SCC-131 cell viability (Table 8). The negative coefficient is consistent with an overall tendency for viability to decrease at higher treatment concentrations, although individual measurements vary across the tested concentrations.

Table 8. Reported Pearson Correlation Between PDEN Concentration and SCC-131 Cell Viability.

Statistical measure	Reported value
Pearson correlation coefficient (r)	−0.630

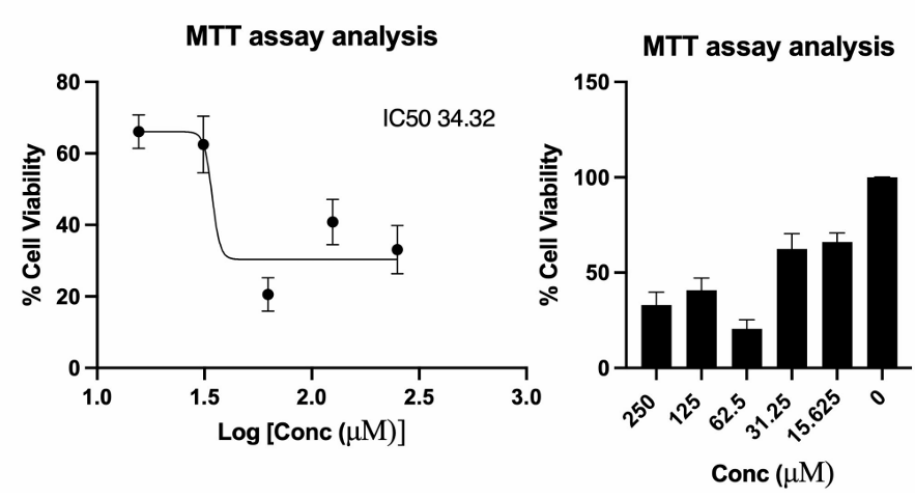


Figure 9. Dose–response relationship between papaya leaf-derived PDEN concentration and SCC-131 cell viability as assessed by the MTT assay. The reported IC_{50} is 34.32 µg/mL. Data presentation should include the mean ± SEM and the number of replicates once verified against the original measurements.

4. DISCUSSION

4.1. Comparison of PEG Precipitation Conditions

This study compared nine PEG-based precipitation conditions to evaluate their associated protein and lipid recovery and identify a preparation for further characterization and biological testing. Protein and lipid concentrations varied with PEG molecular weight and concentration, indicating that the recovered preparation's composition depended on the precipitation condition.

The highest protein concentration was obtained with 8 kDa PEG at 12% (w/v), but this preparation also had a relatively high P/L ratio of 4.47. In contrast, the 8 kDa PEG 6% preparation had a P/L ratio of 2.91 and a reported protein concentration of 4,004.5 µg/mL. These measurements show that maximizing measured protein concentration did not necessarily yield the lowest P/L ratio.

PEG precipitation is a practical method for enriching extracellular-vesicle preparations, but co-precipitation of non-vesicular proteins remains a recognized limitation. PEG molecular weight and concentration, along with the starting material and subsequent purification steps, can affect the composition of the recovered fraction (Farhang Aliakbari et al., 2024; Marzouk et al., 2025). Protein-to-lipid ratio can therefore serve as a comparative measure of preparation composition, although it cannot independently demonstrate vesicle purity or structural integrity (Osteikoetxea et al., 2015).

An important qualification arises from the present dataset: the 6 kDa PEG 6% preparation had the lowest reported P/L ratio, at 2.76, compared with 2.91 for 8 kDa PEG 6%. Consequently, the 8 kDa PEG 6% formulation should not be

described as the condition with the lowest P/L ratio. It was the preparation subsequently selected for characterization and cell-based testing, but the basis for preferring it over the 6 kDa PEG 6% formulation should be stated in relation to additional selection criteria supported by the experimental record.

4.2. Particle Size Distribution and Surface Charge

The selected preparation had a reported median particle diameter of 133.4 nm and a mean diameter of 154.0 ± 84.4 nm. The two reported size populations, centered at 127.6 and 97.8 nm, indicate heterogeneity in the measured particle population. The span value of 1.4 and the reported peak widths also indicate that the preparation contained particles distributed over a range of sizes rather than a single narrowly defined population.

Particle-size measurements alone do not establish that all detected particles are intact PDENs. NTA measures particle movement in suspension and estimates size and concentration; the measured population may include other particles that contribute to light scattering. Accordingly, these measurements support a nanoscale particle preparation, but definitive vesicle identification requires additional structural or molecular characterization. Huang et al. (2021) and Farhang Aliakbari et al. (2024) discussed approaches to plant extracellular-vesicle isolation and characterization, including the limitations of different methods.

The selected preparation also exhibited a mean zeta potential of −30.73 mV, with a predominant reported population centered at −30.0 mV. This distribution indicates that most measured particles shared a similar negative surface-charge profile. Surface charge may contribute to electrostatic repulsion between particles in suspension, but zeta potential should not be interpreted in isolation as proof of long-term colloidal stability. The investigation did not include a time-course stability assessment or a comparison of aggregation under different storage and buffer conditions.

The NTA and zeta potential results provide complementary physicochemical information for the selected preparation. Nevertheless, the measurements alone do not fully establish its purity, membrane structure, molecular cargo, or biological mechanism. These distinctions matter when interpreting PEG-enriched plant-derived nanoparticles as PDEN preparations rather than as a fully characterized vesicle population.

4.3. Protein Quantification of the Selected Preparation

A fresh batch of the selected 8 kDa PEG 6% preparation was produced to obtain sufficient material for subsequent analysis. The individual measurement visible in the corresponding table is 13,314.5 µg/mL, with an optical density of 2.67.

The increase relative to the protein concentration recorded during the initial formulation comparison may reflect differences between preparations or the quantity and composition of the initial plant extract. However, the provided data are insufficient to determine the cause. Because the number of independent batches, individual replicate measurements, and associated variability are not fully tabulated, the reported difference should not be interpreted as evidence of improved isolation efficiency without further supporting measurements.

A complete record of the individual protein assay results, including standard-curve information, replicate measurements, and blank correction, would allow a more reliable comparison between the initial and subsequent preparations. Protein concentration helps standardize PDEN treatments, but it does not directly indicate particle recovery or vesicle purity.

4.4. Effects on SCC-131 Cell Viability

The MTT assay was used to evaluate the effect of the selected papaya leaf-derived PDEN preparation on SCC-131 oral squamous cell carcinoma cells. Several treatment groups showed lower reported viability than the medium-only control. The investigation reports an IC_{50} of 34.32 µg/mL based on dose–response analysis.

However, the individual viability data show a non-monotonic pattern. In particular, the reported viability of 20.59% at 62.5 µg/mL is lower than the reported viability of 40.85% at 125 µg/mL and 33.11% at 250 µg/mL. This departure from a simple concentration-dependent response limits the strength of conclusions that can be drawn from the individual treatment values without rechecking the raw data and the fitted model.

The reported Pearson correlation coefficient of −0.630 suggests an overall negative association between concentration and viability, but the coefficient alone does not establish statistical significance. The underlying replicate-level measurements, the precise statistical procedure, and the associated p-value should be provided if conclusions about the strength and significance of the relationship are to be made.

4.5. Morphological Changes Following PDEN Treatment

Microscopic observation of SCC-131 cells after treatment reportedly showed cell rounding, loss of the elongated morphology, reduced attachment to neighboring cells, and an increase in floating cells. These changes were described as more pronounced at higher treatment concentrations and were presented alongside the MTT findings as qualitative evidence of altered cell condition.

Cell rounding and detachment can occur during several forms of cellular stress and cell death. Although such changes may be compatible with apoptosis, morphology alone cannot confirm an apoptotic mechanism. Elmore (2007) describes apoptosis as a regulated process requiring more specific cellular and biochemical evidence. Because the present study reports MTT and morphological assessments but no apoptosis-specific assay, the observed changes should be described as morphological alterations associated with cytotoxic stress rather than definitive proof of apoptosis.

4.6. Comparison with Previous Studies of Carica papaya

The results can be considered alongside previous studies investigating the effects of conventional Carica papaya leaf extracts on cancer cells. Nisa et al. (2016) investigated aqueous leaf extract against MCF-7 breast cancer cells and reported an IC_{50} of 1,319.25 µg/mL in the source manuscript. Priyadurairaj et al. (2020) examined an ethanolic leaf extract against PA-1 human ovarian cancer cells and reported an IC_{50} of 100 µg/mL. In the present study, the reported IC_{50} for the PEG-isolated leaf-derived preparation against SCC-131 cells was 34.32 µg/mL.

These values should not be used to conclude that the isolated preparation is intrinsically more potent than the conventional extracts. The studies use different cellular models, preparations, and experimental conditions, and the concentrations are not necessarily normalized on a comparable basis. In addition, the present MTT data require verification because the

viability pattern is non-monotonic. Direct comparisons therefore remain descriptive rather than evidence of relative therapeutic potency.

Rebeea et al. (2025) reported cytotoxicity-associated morphological changes following treatment of MDA-MB-231 breast cancer cells with C. papaya fruit-peel preparations. Although this provides a broader point of comparison for reported papaya-derived preparations, fruit-peel preparations and leaf-derived PDEN-enriched fractions are not equivalent materials. Differences in source tissue, preparation method, constituent composition, cell line, and experimental conditions should be considered when comparing the findings.

4.7. Limitations and Further Characterization

The current study describes PEG-based isolation and an initial biochemical and physicochemical characterization of papaya leaf-derived particles, followed by in vitro evaluation in SCC-131 cells. The available measurements support further investigation of the preparation, but several limitations should be considered.

First, protein-to-lipid ratio, NTA, and zeta potential do not independently confirm vesicle identity or exclude co-isolated material. Additional structural and molecular characterization is needed to define the particle population better. Second, the available MTT values show a non-monotonic response and incomplete replicate-level presentation, limiting interpretation of the dose–response relationship and the IC_{50} estimate. Third, the observed morphological changes alone do not establish an apoptotic mechanism.

The present findings should therefore be regarded as initial evidence of measurable effects on SCC-131 cell viability under the reported in vitro conditions. Confirming the dose–response pattern, fully reporting replicate-level statistics, and providing additional characterization would strengthen the conclusions. Mechanistic assays and subsequent in vivo evaluation are needed before making claims about the mechanism of action, therapeutic safety, or clinical applicability.

Overall, the manuscript reports successful recovery of a PEG-enriched papaya leaf-derived nanoparticle preparation, measurable physicochemical characteristics, and reduced SCC-131 cell viability in the MTT assay. The strength of these findings depends on resolving the data and reporting inconsistencies identified above.

5. CONCLUSION

This study investigated the isolation, characterization, and in vitro anticancer activity of plant-derived exosome-like nanoparticles (PDENs) from Carica papaya L. leaves using polyethylene glycol (PEG)-based precipitation. Nine combinations of PEG molecular weight and concentration were evaluated by comparing their protein and lipid content and the resulting protein-to-lipid ratios. The 8 kDa PEG formulation at 6% (w/v) was selected for further characterization and biological evaluation.

Nanoparticle tracking analysis of the selected preparation showed a median particle diameter of 133.4 nm and a mean diameter of 154.0 ± 84.4 nm. Zeta potential analysis yielded a mean value of −30.73 mV, with the predominant measured population centered at −30.0 mV. These results describe the particle-size distribution and surface-charge characteristics of the isolated preparation. However, additional structural and molecular characterization is needed to confirm vesicle identity and more comprehensively assess preparation purity.

Evaluation using the MTT assay indicated reduced SCC-131 oral squamous cell carcinoma cell viability following treatment with the papaya leaf-derived preparation. The source analysis reported an IC_{50} of 34.32 μg/mL, while microscopic observations showed cell rounding, reduced adhesion, and an increase in floating cells. These findings indicate measurable in vitro effects under the experimental conditions used; however, the irregular response across some treatment concentrations warrants verification of the underlying measurements and dose–response analysis.

Overall, the study demonstrates the feasibility of using PEG-based precipitation to obtain a papaya leaf-derived nanoparticle preparation for physicochemical characterization and preliminary in vitro evaluation. The findings provide a basis for further investigation but do not yet establish a specific mechanism of action or therapeutic efficacy. Future work should verify and replicate the dose–response results, add structural and molecular characterization, include apoptosis-specific and mechanistic assays, and conduct in vivo evaluation to assess the biological activity, safety, and potential applications of these nanoparticles in oral squamous cell carcinoma.

REFERENCES

1. Alzahrani, F., Khan, M. I., Kameli, N., Alsahafi, E., & Riza, Y. M. (2023). Plant-derived extracellular vesicles and their exciting potential as the future of next-generation drug delivery. Biomolecules, 13(5), Article 839. https://doi.org/10.3390/biom13050839
2. Anusha, R., Ashin, M., & Priya, S. (2023). Ginger exosome-like nanoparticles (GELNs) induced apoptosis, cell cycle arrest, and anti-metastatic effects in triple-negative breast cancer MDA-MB-231 cells. Food and Chemical Toxicology, 182, Article 114102. https://doi.org/10.1016/j.fct.2023.114102
3. Calzoni, E., Bertoldi, A., Cusumano, G., Buratta, S., Urbanelli, L., & Emiliani, C. (2024). Plant-derived extracellular vesicles: Natural nanocarriers for biotechnological drugs. Processes, 12(12), Article 2938. https://doi.org/10.3390/pr12122938
4. C. Research Team. (2026, February 4). Ultimate guide to optimal cell seeding density for MTT assays (96-well plate). Clyte. https://www.clyte.tech/post/ultimate-guide-to-optimal-cell-seeding-density-for-mtt-assays-96-well-plate
5. Dziedzic, A., Kubina, R., Bułdak, R., Skonieczna, M., & Cholewa, K. (2016). Silver nanoparticles exhibit the dose-dependent anti-proliferative effect against human squamous carcinoma cells attenuated in the presence of berberine. Molecules, 21(3), Article 365. https://doi.org/10.3390/molecules21030365
6. Elmore, S. (2007). Apoptosis: A review of programmed cell death. Toxicologic Pathology, 35(4), 495–516. https://doi.org/10.1080/01926230701320337

7. Eloranta, R., Vilén, S.-T., Keinänen, A., Salo, T., Qannam, A., Bello, I. O., & Snäll, J. (2024). Oral squamous cell carcinoma: Effect of tobacco and alcohol on cancer location. Tobacco Induced Diseases, 22, 1–9. https://doi.org/10.18332/tid/189303
8. Farhang Aliakbari, F., Stocek, N. B., Cole-André, M., Gomes, J., Fanchini, G., Pasternak, S. H., Christiansen, G., Morshedi, D., Volkening, K., & Strong, M. J. (2024). A methodological primer of extracellular vesicles isolation and characterization via different techniques. Biology Methods and Protocols, 9(1), Article bpae009. https://doi.org/10.1093/biomethods/bpae009
9. Hariono, M., Julianus, J., Djunarko, I., Hidayat, I., Adelya, L., Indayani, F., Auw, Z., Namba, G., & Hariyono, P. (2021). The future of Carica papaya leaf extract as an herbal medicine product. Molecules, 26(22), Article 6922. https://doi.org/10.3390/molecules26226922
10. Honorato, L., Bonilla, J. J. A., Valdez, A. F., Reis, F. C. G. D., Kornetz, J., Sabino, A. L. R. do N., Rodrigues, M. L., Nosanchuk, J. D., & Nimrichter, L. (2025). Impact of storage on the stability and the protective effect of extracellular vesicles released by Candida albicans. Applied and Environmental Microbiology, 91(12), Article e0169225. https://doi.org/10.1128/aem.01692-25
11. Huang, Y., Wang, S., Cai, Q., & Jin, H. (2021). Effective methods for isolation and purification of extracellular vesicles from plants. Journal of Integrative Plant Biology, 63(12), 2020–2030. https://doi.org/10.1111/jipb.13181
12. Imbesi Bellantoni, M., Picciolo, G., Pirrotta, I., Irrera, N., Vaccaro, M., Vaccaro, F., Squadrito, F., & Pallio, G. (2023). Oral cavity squamous cell carcinoma: An update of the pharmacological treatment. Biomedicines, 11(4), Article 1112. https://doi.org/10.3390/biomedicines11041112
13. Iriawati, I., Vitasasti, S., Rahmadian, F. N. A., & Barlian, A. (2024). Isolation and characterization of plant-derived exosome-like nanoparticles from Carica papaya L. fruit and their potential as anti-inflammatory agent. PLOS ONE, 19(7), Article e0304335. https://doi.org/10.1371/journal.pone.0304335
14. Kalarikkal, S. P., Prasad, D., Kasiappan, R., Chaudhari, S. R., & Sundaram, G. M. (2020). A cost-effective polyethylene glycol-based method for the isolation of functional edible nanoparticles from ginger rhizomes. Scientific Reports, 10, Article 4456. https://doi.org/10.1038/s41598-020-61358-8
15. Kumar, M., & Jha, A. K. (2023, October 4). Exploring the potential of dietary factors and plant extracts as chemopreventive agents in oral squamous cell carcinoma treatment. PubMed Central. https://pmc.ncbi.nlm.nih.gov/articles/PMC10582632/
16. Langellotto, M. D., Rassu, G., Serri, C., Demartis, S., Giunchedi, P., & Gavini, E. (2024). Plant-derived extracellular vesicles: A synergetic combination of a drug delivery system and a source of natural bioactive compounds. Drug Delivery and Translational Research. https://doi.org/10.1007/s13346-024-01698-4
17. Li, P., Kaslan, M., Lee, S. H., Yao, J., & Gao, Z. (2017). Progress in exosome isolation techniques. Theranostics, 7(3), 789–804. https://doi.org/10.7150/thno.18133
18. Liu, D., Gao, J., Wu, X., & Han, L. (2025). Plant-derived exosome-like nanoparticles as promising biotherapeutic tools: Recent advances and challenges. Smart Materials in Medicine, 6(2), 285–304. https://doi.org/10.1016/j.smaim.2025.07.003
19. Mansoury, M., Hamed, M., Karmustaji, R., Al Hannan, F., & Safrany, S. T. (2021). The edge effect: A global problem. The trouble with culturing cells in 96-well plates. Biochemistry and Biophysics Reports, 26, Article 100987. https://doi.org/10.1016/j.bbrep.2021.100987
20. Maruthanila, V. L., Elancheran, R., & Mirunalini, S. (2020). Carica papaya leaves and cancer prevention: An overview. Mini-Reviews in Medicinal Chemistry, 20. https://doi.org/10.2174/1389557520666200811102622
21. Marzouk, R. M., Gab-Allah, M. A., & Kim, J. (2025). Polyethylene glycol (PEG)-based precipitation for exosome enrichment: A review on recent developments, current challenges, and future perspectives. Analytical Science and Technology, 38(2), 42–64. https://doi.org/10.5806/AST.2025.38.2.42
22. Munir, S., Liu, Z.-W., Tariq, T., Rabail, R., Kowalczewski, P. Ł., Lewandowicz, J., Blecharczyk, A., Abid, M., Inam-Ur-Raheem, M., & Aadil, R. M. (2022). Delving into the therapeutic potential of Carica papaya leaf against thrombocytopenia. Molecules, 27(9), Article 2760. https://doi.org/10.3390/molecules27092760
23. Nisa, F. Z., Astuti, M., Murdiati, A., & Mubarika, H. S. (2016). Anti-proliferation and apoptosis induction of aqueous leaf extract of Carica papaya L. on human breast cancer cells MCF-7. Pakistan Journal of Biological Sciences, 20(1), 36–41. https://doi.org/10.3923/pjbs.2017.36.41
24. Ojong, C., Besong, S. A., & Aryee, A. N. A. (2026). Solvent-based extraction recovers phytochemicals from medicinal plants demonstrating anticancer and chemopreventive potential: A review. Molecules, 31(7), Article 1202. https://doi.org/10.3390/molecules31071202
25. Oral Cancer Foundation. (2019). Mucositis. https://oralcancerfoundation.org/complications/mucositis/
26. Osteikoetxea, X., Balogh, A., Szabó-Taylor, K., Németh, A., Szabó, T. G., Pálóczi, K., Sódar, B., Kittel, Á., György, B., Pállinger, É., Matkó, J., & Buzás, E. I. (2015). Improved characterization of EV preparations based on protein to lipid ratio and lipid properties. PLOS ONE, 10(3), Article e0121184. https://doi.org/10.1371/journal.pone.0121184
27. Priyadurairaj, R., Reddy, P. R. K., Thiruvanavukkarasu, P., & Rajesh, S. (2020). Effect of ethanolic extract of Carica papaya leaves and their cytotoxicity and apoptotic potential in human ovarian cancer cell lines—PA-1. Pharmacognosy Magazine, 16(5), 524–530. https://phcog.com/article/view/2020/16/05/524-530
28. Ramsridhar, S., Rajkumar, C., Veeraraghavan, V. P., Prakash Francis, A., Balasubramaniam, M., & Bharkavi, I. (2025). From cell lines to animal models: "Plant-derived chemotherapeutics unlocking new frontiers against oral squamous cell carcinoma"—A comprehensive systematic review. Discover Oncology, 16, Article 340. https://doi.org/10.1007/s12672-025-02057-6

29. Rebeea, V. M., Muhsina, A., Rameesa, M., Fathima, H. S., Shani, T., Ashik, T., Shanmugavelu, V. K., & Suhail, P. (2025). Identification of phytochemicals and evaluation of anticancer activity of peels of Carica papaya fruit. Journal of Research in Pharmacy, 29(5), 2143–2150. https://doi.org/10.12991/jrespharm.1766388
30. Rider, M. A., Hurwitz, S. N., & Meckes, D. G., Jr. (2016). ExtraPEG: A polyethylene glycol-based method for enrichment of extracellular vesicles. Scientific Reports, 6, Article 23978. https://pmc.ncbi.nlm.nih.gov/articles/PMC4828635/
31. Sankar, V., & Xu, Y. (2023). Oral complications from oropharyngeal cancer therapy. Cancers, 15(18), Article 4548. https://doi.org/10.3390/cancers15184548
32. Sharma, A., Sharma, R., Sharma, M., Kumar, M., Barbhai, M. D., Lorenzo, J. M., Sharma, S., Samota, M. K., Atanassova, M., Caruso, G., Naushad, M., Radha, Chandran, D., Prakash, P., Hasan, M., Rais, N., Dey, A., Mahato, D. K., Dhumal, S., & Singh, S. (2022). Carica papaya L. leaves: Deciphering its antioxidant bioactives, biological activities, innovative products, and safety aspects. Oxidative Medicine and Cellular Longevity, 2022, Article 2451733. https://doi.org/10.1155/2022/2451733
33. Shkryl, Y., Tsydeneshieva, Z., Menchinskaya, E., Rusapetova, T., Grishchenko, O., Mironova, A., Bulgakov, D., Gorpenchenko, T., Kazarin, V., Tchernoded, G., Bulgakov, V., Aminin, D., & Yugay, Y. (2024). Exosome-like nanoparticles, high in trans-δ-viniferin derivatives, produced from grape cell cultures: Preparation, characterization, and anticancer properties. Biomedicines, 12(9), Article 2142. https://doi.org/10.3390/biomedicines12092142
34. Srinivasan, S., Muthukumar, R. S., & Nachiappan, N. N. (2025, September 26). Evaluation of cytotoxic effects of fruit extracts on oral cancer cell lines: An in vitro experimental study. PubMed Central. https://pmc.ncbi.nlm.nih.gov/articles/PMC12507376/
35. Suharta, S., Barlian, A., Hidajah, A. C., Notobroto, H. B., Ana, I. D., Indariani, S., Wungu, T. D. K., & Wijaya, C. H. (2021). Plant-derived exosome-like nanoparticles: A concise review on its extraction methods, content, bioactivities, and potential as functional food ingredients. Journal of Food Science, 86(7), 2838–2850. https://doi.org/10.1111/1750-3841.15787
36. Tan, Y., Wang, Z., Xu, M., Li, B., Huang, Z., Qin, S., Nice, E. C., Tang, J., & Huang, C. (2023). Oral squamous cell carcinomas: State of the field and emerging directions. International Journal of Oral Science, 15(1). https://doi.org/10.1038/s41368-023-00249-w
37. Thermo Fisher Scientific. (n.d.). BCA protein assays. https://www.thermofisher.com/us/en/home/life-science/protein-biology/protein-assays-analysis/protein-assays/bca-protein-assays.html
38. Théry, C., Amigorena, S., Raposo, G., & Clayton, A. (2006). Isolation and characterization of exosomes from cell culture supernatants and biological fluids. Current Protocols in Cell Biology, 30(1), Unit 3.22. https://doi.org/10.1002/0471143030.cb0322s30
39. Vikas, B., & Anil, S. (2020). Cell-based assays in cancer research. IntechOpen. https://doi.org/10.5772/intechopen.90226
40. World Health Organization. (2025a, February 3). Cancer. https://www.who.int/news-room/fact-sheets/detail/cancer
41. World Health Organization. (2025b). Oral health. https://www.who.int/news-room/fact-sheets/detail/oral-health
42. Xu, J. Y., Xiao, Y. L., & Yu, Z. L. (2026). From biomedical mechanisms to clinical applications: Research progress in plant-derived vesicles for cancer therapy. International Journal of Nanomedicine, 21, Article 573022. https://doi.org/10.2147/IJN.S573022
43. Yang, M., Luo, Q., Chen, X., & Chen, F. (2021). Bitter melon-derived extracellular vesicles enhance the therapeutic effects and reduce the drug resistance of 5-fluorouracil on oral squamous cell carcinoma. Journal of Nanobiotechnology, 19(1). https://doi.org/10.1186/s12951-021-00995-1
44. Zhan, M., Zhao, C., Han, Y., & Xiao, H. (2026). From isolation to function: A review of plant-derived exosome-like nanoparticles. Trends in Food Science & Technology, 171, Article 105643. https://doi.org/10.1016/j.tifs.2026.105643
45. Zhang, J., Zuo, Y., Sun, B., Wang, X., Tian, S., & Miao, M. (2026). Plant-derived vesicle-like nanoparticles for cancer therapy: From drug delivery to combined immunotherapy. Antioxidants, 15(3), Article 311. https://doi.org/10.3390/antiox15030311